JACS
JOURNAL OF THE AMERICAN CHEMICAL SOCIETY
pubs.acs.org/JACS

Article

High Molar Mass Polycarbonates as Closed-Loop Recyclable Thermoplastics

Gloria Rosetto, Fernando Vidal, Thomas M. McGuire, Ryan W. F. Kerr, and Charlotte K. Williams*

Cite This: J. Am. Chem. Soc. 2024, 146, 8381−8393

Read Online

ACCESS | Metrics & More | Article Recommendations | Supporting Information

ABSTRACT: Using carbon dioxide (CO_2) to make recyclable thermoplastics could reduce greenhouse gas emissions associated with polymer manufacturing. CO_2/cyclic epoxide ring-opening copolymerization (ROCOP) allows for >30 wt % of the polycarbonate to derive from CO_2; so far, the field has largely focused on oligocarbonates. In contrast, efficient catalysts for high molar mass polycarbonates are underinvestigated, and the resulting thermoplastic structure−property relationships, processing, and recycling need to be elucidated. This work describes a new organometallic Mg(II)Co(II) catalyst that combines high productivity, low loading tolerance, and the highest polymerization control to yield polycarbonates with number average molecular weight (M_n) values from 4 to 130 kg mol^{-1}, with narrow, monomodal distributions. It is used in the ROCOP of CO_2 with bicyclic epoxides to produce a series of samples, each with M_n > 100 kg mol^{-1}, of poly(cyclohexene carbonate) (PCHC), poly(vinyl-cyclohexene carbonate) (PvCHC), poly(ethyl-cyclohexene carbonate) (PeCHC, by hydrogenation of PvCHC), and poly(cyclopentene carbonate) (PCPC). All these materials are amorphous thermoplastics, with high glass transition temperatures (85 < T_g < 126 °C, by differential scanning calorimetry) and high thermal stability (T_d > 260 °C). The cyclic ring substituents mediate the materials' chain entanglements, viscosity, and glass transition temperatures. Specifically, PCPC was found to have 10× lower entanglement molecular weight $(M_e)_n$ and 100× lower zero-shear viscosity compared to those of PCHC, showing potential as a future thermoplastic. All these high molecular weight polymers are fully recyclable, either by reprocessing or by using the Mg(II)Co(II) catalyst for highly selective depolymerizations to epoxides and CO_2. PCPC shows the fastest depolymerization rates, achieving an activity of 2500 h^{-1} and >99% selectivity for cyclopentene oxide and CO_2.

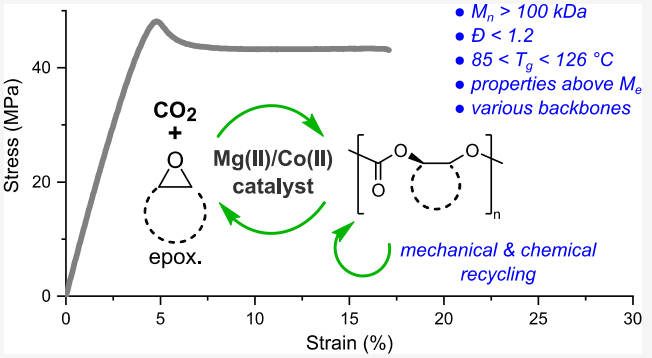

INTRODUCTION

Polymers are among the largest scale chemicals produced; they are currently manufactured at a rate of around 400 megatonnes (Mt) annually.[1−3] Their production from petrochemicals accounts for >1.0 gigatonne of carbon dioxide-equivalents (Gt CO_2-equiv), representing >60% of overall lifecycle emissions. The total carbon footprint and other environmental pollution is exacerbated by a lack of effective recycling.[3−5] Two important strategies to address these issues have emerged from several recent independent global plastics systemic models: (1) replace virgin petrochemical feedstocks with carbon dioxide utilization technologies, either directly achieved by CO_2-based chemistries or through biomass upgrading and (2) drastically increase thermoplastic recycling rates, ensuring all future materials undergo energy-efficient mechanical recycling and/or chemical recycling to monomers.[1,2,6−10] Our interest is to produce polycarbonate thermoplastics directly using CO_2, showing useful properties and selective end-life recycling (both mechanical and chemical).[7−9]

CO_2 and epoxide ring-opening copolymerization (ROCOP) is a front-runner carbon dioxide utilization technology.[11−13] Most polymerizations apply catalysts to produce hydroxyl telechelic oligocarbonates (1 < M_n < 20 kg mol^{-1}, where M_n is the number average molecular weight), or CO_2-polyols, which are important as surfactants and in production of polyurethane foams, elastomers, coatings, sealants, and adhesives.[13−18] Some excellent catalysts include Co(III) or Al(III) complexes tethered to ionic cocatalysts (often bis(triphenylphosphine)-iminium halides, e.g., PPNCl); dimeric/dinuclear complexes, e.g., Zn(II)Zn(II), Zn(II)Mg(II), Co(II)Mg(II), Ln(III)Zn-(II), which operate without any cocatalyst; or borane complexes tethered to/used with ionic cocatalysts (ammonium or phosphonium halides).[19−41] Such CO_2-polyol catalysts need to be applied with a very large-excess (10−100 equiv vs

Received: December 14, 2023
Revised: February 19, 2024
Accepted: February 22, 2024
Published: March 14, 2024

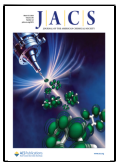

https://doi.org/10.1021/jacs.3c14170
J. Am. Chem. Soc. 2024, 146, 8381−8393

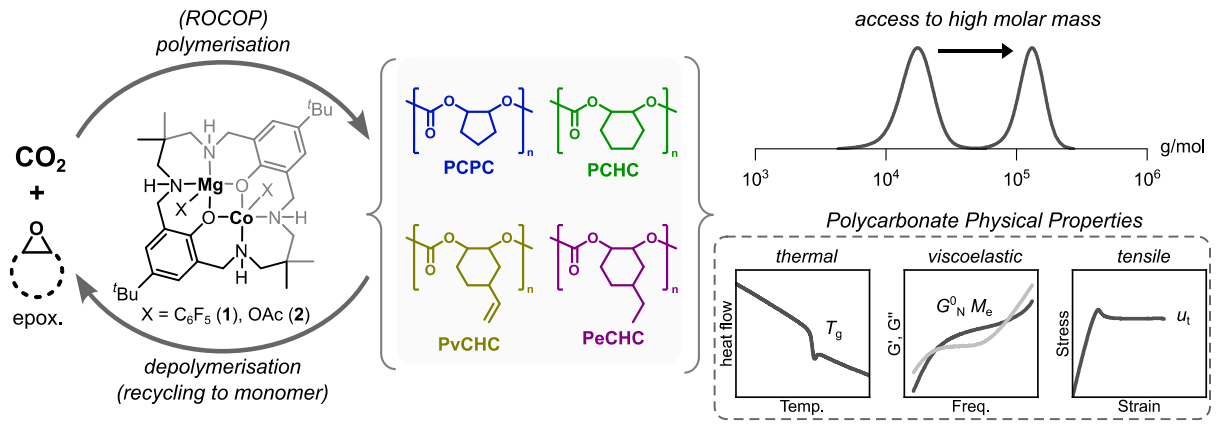

Figure 1. Catalysts and polymers targeted in this work, with the objective of elucidating thermal-mechanical properties and recycling routes for high molarmass cyclic substituted polycarbonates.

catalyst) of a protic chain transfer agent (CTA), often a diol, which controls the oligomer chain length and hydroxyl chain end-groups.[42] Chain transfer reactions are alcoholysis processes, whereby all alcohol groups react rapidly with the growing polymer chains, moving them rapidly on/off the catalyst; these processes generally occur faster than propagation.[27,43,44] Most catalysts also react with residual water, either in the apparatus or monomers, to ring-open epoxides and generate diols in situ, which are also bifunctional CTAs. With the inclusion of these added (or inadvertent) mono- and bifunctional CTAs, together with catalysts or cocatalysts featuring a monofunctional initiator (usually an acetate or chloride), the polymer molar masses almost inevitably exhibit bimodal distributions.[42,44] These restrictions on molar masses, where the M_n is well below the entanglement molecular weight (M_e), and high dispersities ($Đ$) have so far hampered CO_2-based polymers from effectively challenging petroleum-based commodity thermoplastics. For instance, prior studies of poly(cyclohexene carbonate) (PCHC) have consistently noted its difficult processability and high brittleness.[45,46]

In contrast, catalysts that yield high molar mass polycarbonates (M_n = 50−150 kg mol^{-1}) with narrow, monomodal molar mass distributions are much less common.[38,47−49] Accessing such materials is desirable since entanglement phenomena directly impact many polymer physical properties, including glass transition temperature (T_g), crystallization, mechanical strength, and processability.[50] In 2001, Darensbourg and Koning reported upon a moderate molar mass PCHC sample (M_n = 42 kg mol^{-1}, $Đ$ = 6), produced using a Zn(II)Zn(II) catalyst, which showed a tensile stress of 43 MPa, Young's modulus of 3.3 GPa, but only 2% elongation at break.[45] The authors estimated an M_e of ∼15 kg mol^{-1} but noted that it was likely an underestimation. In 2022, Frey and Floudas investigated, both experimentally and computationally, the chain dynamics of moderate molar mass PCHC (5 < M_n < 33 kg mol^{-1}) produced using a [(*R*,*R*-salcy)CoCl]/PPNCl catalyst system, estimating an M_e of 16 kg mol^{-1}.[46] It is also relevant to note that PCHC has been successfully applied as a "rigid" block in various phase separated copolymers (T_g of PCHC ∼ 110−120 °C), producing adhesives, elastomers, and plastics, depending on the comonomers and overall molar mass values.[15,18,43,51−53] Beyond CHO as comonomer in ROCOP, the teams of Rieger and Greiner independently focused on related 6-membered ring, biobased poly(limonene carbonate), developing routes to high molar mass and terpolymers with PCHC.[54−56] Wu and co-workers reported poly(cyclopentene carbonate) (PCPC) with molar masses up to 84 kg mol^{-1}, but the analyzed sample (M_n = 20 kg mol^{-1}, T_g = 70 °C) displayed moderate tensile strength (20 MPa) and no yield point.[48]

Underpinning future progress on CO_2-based polycarbonates should be informed upon comprehensive material investigations, for instance, by determining the M_e more accurately. To increase the molar mass, two approaches to synthesize PCHC have been proposed. One consists of attempting to rigorously remove all residual protic impurities and traces of water with highly reactive scavengers; however, such purifications might be rather challenging to scale.[47] For instance, Jia and co-workers discovered highly active borane/PPNCl catalysts for CHO/CO_2 ROCOP, which when applied with rigorously dried CO_2 and extensively purified CHO produced PCHC with M_n ∼ 450 kg mol^{-1} ($Đ$ = 1.31). In 2022, Li and co-workers applied the same triethyl borane with different phosphazene cocatalysts to produce high molar mass PCHC (M_n ∼ 280 kg mol^{-1}, $Đ$ = 1.59).[38] These impressive achievements were not accompanied by investigation of the material properties of the polymers. A second strategy applies organometallic catalysts that react in situ with alcohols to form only one type of initiator (the organometallic ligand does not initiate on its own).[47] To reach sufficiently high molar masses, such catalysts must show high activity and tolerate impurities at low loadings. Previously, we reported organometallic Zn(II)Zn(II) and Zn(II)Mg(II) catalysts, which exhibit such initiation control.[43,57,58] Unfortunately, these catalysts were not sufficiently active to produce high molar mass polycarbonates. In 2020, we reported a very active Mg(II)Co(II) acetate catalyst for CHO/CO_2 ROCOP, which is > 1000× faster than Zn(II)Zn(II) and ∼10× faster than Mg(II)Zn(II).[27]

Any future uses for high molar mass CO_2-based plastics must also allow for low-energy recycling options—most obviously by mechanical recycling.[44] In addition, chemical recycling strategies allow for recovery of the constituent monomers, in this case, epoxides and CO_2.[7,59,60]

Darensbourg and co-workers pioneered CO_2-derived polycarbonate chemical recycling, describing the first catalysts, applied with a strong base, for the depolymerization of PCPC to cyclopentene oxide and CO_2.[61] Subsequently, a range of other catalysts were active for PCHC and other cyclic substituted polycarbonates.[62−68] Although promising results have been obtained, the understanding and overall perform-

https://doi.org/10.1021/jacs.3c14170
J. Am. Chem. Soc. 2024, 146, 8381−8393

ance of such depolymerization catalysis require improvements to maximize energy efficiency.

Thus, to address these challenges, we propose to employ a novel non-initiating organometallic Mg(II)Co(II) catalyst (Figure 1). When used with 5- and 6-membered cyclic epoxides, the latter including alkyl substituents (vinyl-and ethyl-cyclohexene), high molar mass CO_2-based polycarbonates with end-group selectivity and narrow dispersity will allow us to elucidate polymer structure−property relationships. Finally, the Mg(II)Co(II) catalyst will also be investigated in depolymerization reactions, targeting high activity, selectivity, minimal catalyst loading, and reducing the operating temperatures for efficient chemical recycling to high-value epoxide monomers and CO_2.

RESULTS

Catalyst Synthesis and Carbon Dioxide ROCOP Catalysis. To investigate the best catalysts for high molar mass polycarbonate production, the organometallic Mg(II)-Co(II) complex (**1**) and previously reported Mg(II)Co(II) diacetate complex (**2**) were compared (Figure 1).[27] Pentafluorophenyl was selected as the organometallic ligand for its anticipated stability (with respect to β-H elimination), high reactivity of Co−C_6F_5 with alcohols to undergo irreversible protonation, and low nucleophilicity of Co−C_6F_5 to prevent CO_2 insertion. These features ensure that the complex is non-initiating, which is essential for high molar mass polymer production. The new organometallic Mg(II)Co(II) catalyst, **1**, was prepared with pentafluorophenyl groups as the hydrolyzable non-initiating coligands. To make the catalyst, the macrocyclic ligand [LH_2] was first reacted with [Mg{N-($SiMe_3$)$_2$}$_2$], followed by a reaction with cobalt(II) bis-(pentafluorophenyl) ([Co(C_6F_5)$_2$ (THF)$_2$]) and stirring the mixture for 24 h.[69,70] Complex **1**, [LMgCo(C_6F_5)$_2$], was isolated by cooling the reaction solution to −30 °C, as a purple crystalline solid, in 53% yield. Complex **2** was prepared following literature methods.[27] Single crystals of **1**, suitable for X-ray diffraction, were isolated via recrystallization, from a saturated THF solution, at −30 °C. Its solid-state structure confirms the formation of a heterodinuclear complex (Figure 2a and Table S1), with the aryl coligands coordinated at each metal and the ligand adopting an "S" shape. In complex **1**, the Co(II) center is pentacoordinate and adopts a distorted square pyramidal geometry with the aryl ligand coordinated at the apex (Figure 2b). The Mg(II)Co(II) separation is 3.069(3) Å (Table S2 for selected bond lengths and angles).

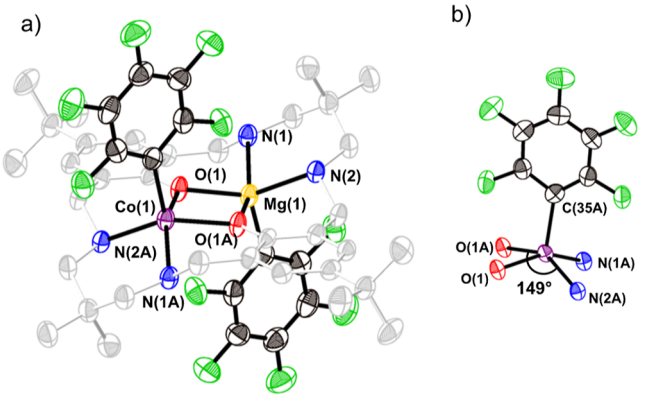

Figure 2. (a) ORTEP diagram for the molecular structure of **1**. H atoms and two THF molecules were omitted for clarity. Thermal ellipsoids are at 50% probability level. Co = purple, Mg = yellow, O = red, N = blue, F = green, C = gray (Figure S1 for full structure, Table S1 for crystallographic details). (b) Section of the crystal structure depicting the square pyramidal geometry around the cobalt center.

The ^{1}H NMR spectrum of complex **1**, in toluene-d_8, shows peaks from −55 to 270 ppm, characteristic of a paramagnetic Co(II) species (Figure S2). Its ^{19}F{^{1}H} NMR spectrum shows three peaks: two broad singlets at −155 and −65 ppm and a triplet at −154 ppm, the relative integrals are 2:1:1 (Figure S4, see the Supporting Information for a discussion on the characterization of **1**). Complex **1** was also characterized by SQUID magnetometry and cyclic voltammetry (CV). The magnetic moment, arising from Co(II), is 4.99 $\mu_{B,}$ which is consistent with a square pyramidal high spin, Co(II) d^7 complex (Figure S6). Previously, Hoffmann and Rossi investigated the structures for related five-coordinate Co(II) complexes, and **1** shows an electronic configuration consistent with their proposal.[71] It also shows an irreversible Co(II/III) oxidation at E_{pa} = −0.819 V (vs Fc/Fc$^+$) and ligand-centered oxidations at E_{pa} = 0.39 V (vs Fc/Fc$^+$) (Figure S7).

To make high molar mass polycarbonates, it is essential to cleanly control the initiation reaction, and here, this is achieved using an organometallic ligand, which reacts with alcohols (CTAs). To investigate the initiation process further, complex **1** (0.01 mmol) was reacted with 2 equiv of 2-fluorophenol at room temperature in toluene-d_8. The reaction was conducted in a Young's tap NMR tube and monitored by spectroscopy (Figure S12). The addition of alcohol resulted in an immediate change of color, from pale to a much brighter pink (Figure S13). The resulting ^{19}F{^{1}H} NMR spectrum showed new resonances at −56 and −132 ppm, corresponding to the clean formation of the new 4-fluorophenoxide ligands coordinated to the Co(II) and Mg(II) centers, respectively. In addition, the product of alcoholysis, HC_6F_5, was also detected with a 1:1 relative integration, further confirming the expected reactivity. This small-scale experiment proves that the reaction between complex **1** and alcohols is instantaneous, quantitative, and irreversible. Such reactivity is essential for initiation control during polymerization, which is required to achieve high molar mass polymers.

Next, the control of epoxide/CO_2 ROCOP with complex **1** was studied using 4 equiv of 1,2-cyclohexane diol (CHD) as CTA and CHO as the comonomer to produce PCHC. MALDI-ToF analysis of a low molar mass PCHC sample, prepared in toluene at 80 °C using a [**1**]:[CHD]:[CHO] ratio of 1:4:2000, pressurized to 1 bar of CO_2 and quenched at low conversions (10 min, conv. ∼5%), shows a single distribution of α,ω-dihydroxy telechelic polymer chains, initiated solely from CHD (Figure 3b). There was no evidence of any chains initiated by pentafluorophenyl groups or from carboxylates formed by carbon dioxide insertion (Figure S14 for end group calculations). In contrast, complex **2**, under identical conditions, generates polymer chains displaying both α,ω-dihydroxyl and α-acetal-ω-hydroxy end-groups. The two different end-groups result from a mixture of CHD and non-innocent catalyst acetate groups, respectively (Figure 3a). Another structural feature of note is polymer tacticity, which can be determined by quantitative ^{13}C NMR spectroscopy.[72] The spectrum for a PCHC sample catalyzed by **1** showed that the polymer is atactic, with a P_m value of 0.5 (Figure S15).

Next, vinyl-cyclohexene oxide (vCHO)/CO_2 ROCOP was conducted, at 1 bar pressure, using either catalyst **1** or **2**. The

https://doi.org/10.1021/jacs.3c14170
J. Am. Chem. Soc. 2024, 146, 8381−8393

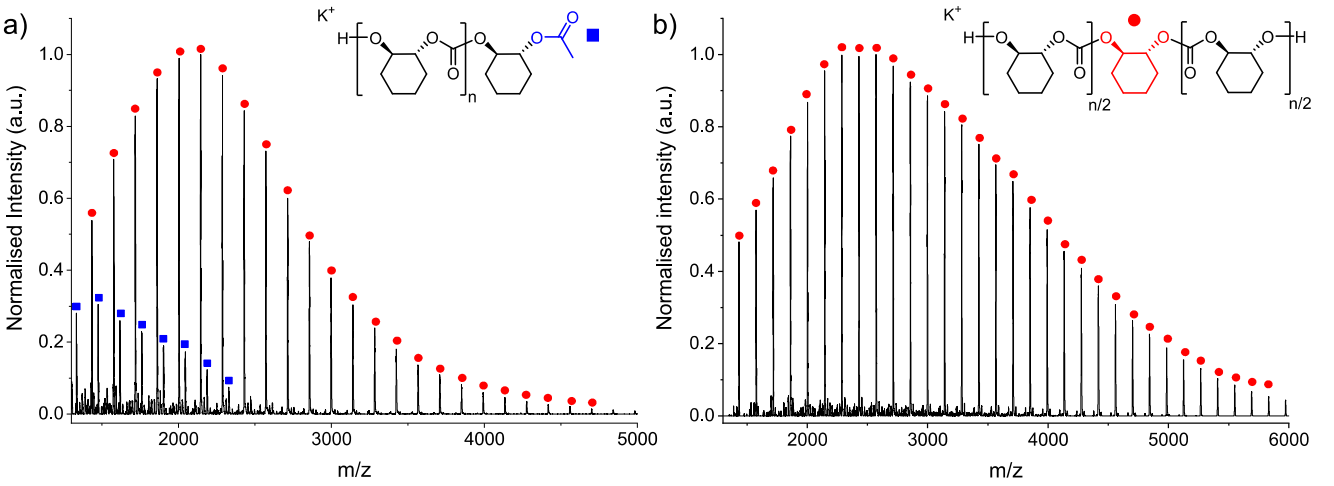

Figure 3. MALDI-ToF spectra for low molar mass samples of PCHC prepared using catalyst **2** (a) or **1** (b). Polymerization conditions: [catalyst]:[CHD]:[CHO] = 1:4:2000, using a solution of 3 M CHO in toluene, 80 °C, quenched after 10 min, conv. ~5%. Chain distributions that are end-capped by CHD are marked with a red circle, and those by acetate are marked with a blue square. See Figure S14 for end group calculations and *m*/*z* peak annotation of MALDI-ToF spectra.

vCHO comonomer was selected since it generally polymerizes at a similar rate to CHO but benefits from an additional alkene substituent on the cyclohexene ring, which might enable postpolymerization functionalization and enable study of pendant alkyl substituents on the dynamics of polymer chains.[17,73−76] Using [**1**]:[CHD]:[vCHO] of 1:4:2000, at 100 °C and 1 bar of CO_2 pressure, the reaction reached 30% epoxide conversion within an hour and formed poly(vinylcyclohexene carbonate) (PvCHC)with >99% carbonate linkage selectivity (Figure S16). Catalyst **1** shows good activity, with a turnover frequency (TOF) of 600 h^{-1}, which is closely comparable to that using **2** (TOF = 660 h^{-1}), under identical conditions.[27] Further, initial rates for these reactions, calculated from CO_2 mass flow data, are also very similar for catalysts **1** and **2**, with k_{obs} values of 4.5 and 4.2 min^{-1}, respectively (Figure S17). These findings demonstrate that the coligands (aryl or acetate) do not influence the polymerization propagation kinetics, i.e., the two catalysts feature virtually identical propagating intermediates.[26,43] The ligands do, however, significantly influence the initiation processes and the resulting molar masses and distributions. Using catalyst **1**, PvCHC has a higher molar mass and monomodal distribution (M_n = 22.2 kg mol^{-1}, $Đ$ = 1.08) (Figure 4a), while, under identical conditions, **2** yields polymers with lower molar mass and bimodal distributions (M_n = 16.7 kg mol^{-1}, $Đ$ = 1.19) (Figure 4b). In the case of catalyst **2**, the bimodality can be deconvoluted into a lower molar mass distribution, assigned to acetate-initiated chains, and a higher molar mass distribution, assigned to CHD-initiated polymer chains (Figure 4b).

Catalyst**1** showed improved polymerization control and was therefore applied using a range of different [catalyst]:[epoxide] ratios to prepare a series of high molar mass polycarbonates. The polymerizations were all performed in toluene solutions of the appropriate epoxide (3.0 M) using steel Parr-reactors, at 20 bar CO_2 pressure; these conditions ensured efficient mixing and stirring particularly as conversion and viscosity increased, enabling maximum productivity (turnover numbers, TON) and high epoxide conversions (Table 1). It is worth noting that typical ROCOP conditions are selected to maximize polymerization rates at low epoxide conversions, where viscosities are low.[77] On the other hand, conditions to achieve high epoxide

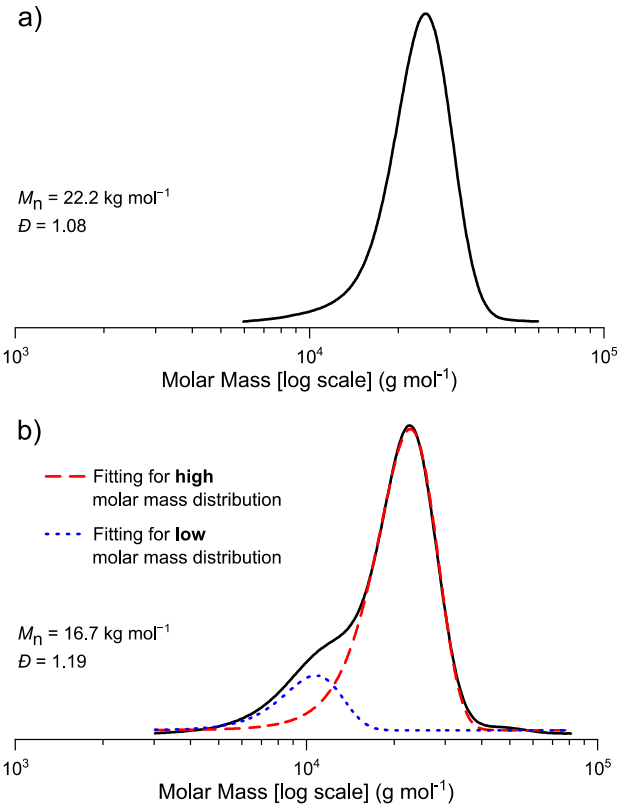

Figure 4. GPC traces of PvCHC (THF as eluent) produced by catalysts **1** (a) and **2** (b), in which case the molar mass peak was deconvoluted into two bimodal distributions as shown by the dashed and point lines. Polymerization conditions: [catalyst]:[CHD]:[vCHO] = 1:4:2000, 1 bar of CO_2, 100 °C, 1 h.

conversion, where viscosities are higher and rates are lower, are comparatively underinvestigated. Since metal-catalyzed epoxide/CO_2 copolymerizations are controlled, high epoxide conversions should result in the highest polymer molar masses. Further, the polymer molar mass should be inversely related to the quantity of CHD added since it functions as both the chain-initiator and chain-transfer agent (Figure S18). To demonstrate the outstanding polymerization control and

https://doi.org/10.1021/jacs.3c14170
J. Am. Chem. Soc. 2024, 146, 8381−8393

Table 1. Data for Bicyclic Epoxide/CO_2 ROCOP Using Catalyst 1[a]

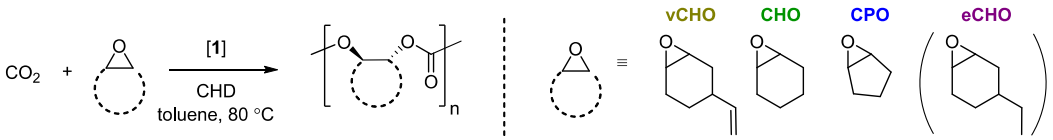

run (#)	polymer	epoxide	CHD equiv	epoxide equiv	time (h)	epoxide conv. (%)[b]	TON[c]	$M_{n,\,GPC}$ (kg mol^{-1})[d]	$Đ$[e]	$M_{n,\,est}$ (kg mol^{-1})[f]
1	PvCHC-16	vCHO	32	3000	10	95	2850	16.0	1.10	14
2	PvCHC-29	vCHO	16	3000	10	99	2970	28.5	1.09	28
3	PvCHC-43	vCHO	8	3000	8	95	2850	43.4	1.10	48
4	PvCHC-82	vCHO	4	3000	10	99	2970	81.9	1.07	84
5	PvCHC-125	vCHO	4	6000	24	99	5940	124.5	1.06	126
6	PvCHC-163	vCHO	4	10,000	30	98	9800	162.8	1.17	153
7	PCHC-122	CHO	4	10,000	18	95	9500	121.6	1.09	333[g]
8	PCPC-114	CPO	4	10,000	40	96	9600	114.4	1.06	320[g]
9	PeCHC-125	eCHO						72.6	1.34	125

[a]Polymerizations were all conducted at 80 °C, 20 bar CO_2 in toluene (3 M solutions of epoxide); PeCHC was produced by hydrogenation of PvCHC (see the Supporting Information for details), monomer structure shown for comparison. [b]Determined by ^{1}H NMR spectroscopy by comparing the integrals of the resonances for the epoxide vs those of the polymer (Figures S24−S26). [c]TON = (moles of epoxide converted)/(moles of catalyst). [d]Determined by GPC, in THF, calibrated using narrow polystyrene standards. [e]$Đ = M_w/M_n$, determined by GPC. [f]$M_{n,\,est}$ = [(epoxide conv.)(epoxide equiv)(MW repeat unit)] + [(CHD equiv)(MW CHD)]/(CHD + x) (where x = residual CTA, see the Supporting Information for further information). [g]$M_{n,\,est}$ = [(epoxide conv.)(epoxide equiv)(MW repeat unit)] + [(CHD equiv)(MW CHD)]/(CHD).

alcohol tolerance of complex **1**, CO_2/epoxide ROCOP was conducted using systematically increasing quantities of CHD (4 to 32 equiv) vs **1**. In these investigations, a [**1**]:[vCHO] loading ratio of 1:3000 (0.033 mol % catalyst) was kept constant, and polymerizations all achieved >95% CHO conversion (Table 1, entries 1−4). Notably, the resulting series of PvCHC samples all show very narrow (1.07 < $Đ$ < 1.10) monomodal molar mass distributions, which are typical of well-controlled polymerizations (Figure 5). The experimentally determined molar mass values, using GPC against polystyrene standards, are high (M_n up to 81.9 kg mol^{-1}) and inversely related to the quantity of CTA added. The catalyst's remarkable tolerance and stability at very low concentrations and high alcohol (CHD) loadings are clear from the good correlation between experimental and theoretical molar masses, $M_{n,\,est}$ (see the Supporting Information for further detail). Further decreasing catalyst loadings to 0.017 mol % and even 0.010 mol %, with constant 4 equiv of CHD, resulted in all cases in almost complete conversions (>95%) to PvCHC (Table 1, entries 5−6). These experiments yielded the target high molar masses of 125 and 163 kg mol^{-1}, with monomodal and narrow $Đ$ (1.06−1.17) (Figure 5). The catalyst's ability to control the molar mass by varying either the catalyst or diol loading, and to achieve complete conversions, is essential to investigate the thermal-mechanical properties of the resulting materials.

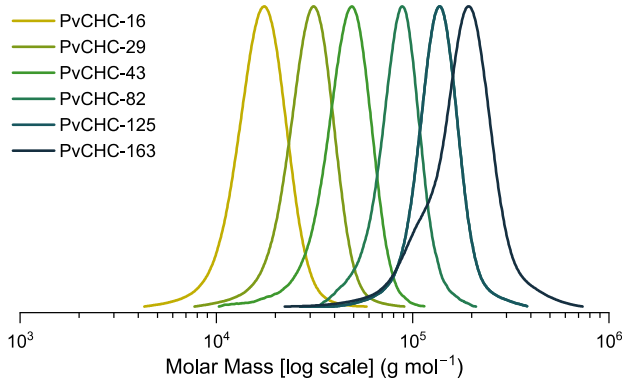

Figure 5. GPC traces (THF as the eluent) of PvCHC samples produced by using catalyst **1** (Table 1). A deconvoluted GPC trace of PvCHC-163 is provided in the Supporting Information (Figure S19) showing that the lower molar mass shoulder accounts for 1.2% of the total distribution.

Having optimized the reaction conditions to reach high molar masses with 0.010 mol % loadings of catalyst **1**, the ROCOP catalysis was extended using cyclohexene oxide (CHO) or cyclopentene oxide (CPO). Similarly, high epoxide conversions, at 80 °C in toluene, produced high molar mass polycarbonates (Table 1, entries 7−8). Specifically, CHO produced PCHC with M_n = 121.6 kg mol^{-1} and very narrow $Đ$ = 1.09 (Figure S20), while CPO produced PCPC with M_n = 114.4 kg mol^{-1} and $Đ$ = 1.06 (Figure S21). Despite these high molar masses, in these cases, there are discrepancies between the experimental and theoretical values, which are attributed to the use of GPC standards and/or different quantities of residual diols in the epoxides.

Hydrogenation of vinyl groups in PvCHC to PeCHC. Finally, to expand our study on the effect of ring size and substituents in CO_2-derived polycarbonates, the potential to modify the alkene of PvCHC was explored. Hydrogenation of the vinyl group was selected since it will yield ethyl substituents on the cyclohexane rings; alkylated polymers are known to be more easily processed. Following a modified literature procedure, PvCHC-125 was reacted with *para*-toluenesulfonyl hydrazide and formed the corresponding alkylated polymer, PeCHC-125, in good yield (68% following repeated precipitation from MeOH).[78] The hydrogenation reaction did not significantly change the polymer backbone, although there was some low molar mass tailing via GPC (M_n = 72.6 kg mol^{-1}, $Đ$ = 1.34) (Figures S22 and S23).

Polycarbonate's Thermal-Mechanical Properties. Any attempts to use these higher-molar-mass polycarbonates as thermoplastics require insights into their thermal and viscoelastic properties since these will control the temperature ranges over which they can be processed and used. The series of ∼120 kg mol^{-1} CO_2-polycarbonates were each characterized

https://doi.org/10.1021/jacs.3c14170
J. Am. Chem. Soc. 2024, 146, 8381−8393

Table 2. Thermal and Viscoelastic Properties of the High Molar Mass Polycarbonates[a]

polymer	$T_{g,DSC}$[c] (°C)	$T_{g,rheo}$[d] (°C)	$T_{t,cross}$[e] (°C)	T_d[f] (°C)[b]	G_{glass}'[g] (MPa)	G_N^0[h] (MPa)	M_e[i] (kg mol^{-1})	τ_t[j] (min)	η_0[k] (MPa s)
PCPC-114	85	97	166	271	453	0.65 ± 0.02	3.4−4.6	0.21 ± 0.02	0.78 ± 0.09
PeCHC-125	105	118	161	306	447	0.170 ± 0.004	13−18	0.57 ± 0.03	1.26 ± 0.11
PvCHC-125[b]	118	129	196	277	459	0.049 ± 0.017	45−62	87 ± 18	30 ± 20
PCHC-122	126	132	192	265	453	0.056 ± 0.011	56	240 ± 30	90 ± 20

[a]Time−temperature superposition (TTS) master curves were referenced at 140 °C (see the Supporting Information for experimental details and calculations, Figures S31−S38). [b]Sample was stabilized with 0.1 wt % of a radical inhibitor, pentaerythritol tetrakis (3,5-di-*tert*-butyl-4-hydroxyhydrocinnamate) (PEHC). [c]Measured by DSC from the second scan at a heating rate of 10 °C·min^{-1} (Figure S27a). [d]Measured by oscillatory shear rheology from the peak in the tan(δ) curve obtained during temperature ramp experiments at heating rates of 2 °C·min^{-1} (Figures S31, S33, S35 and S37). [e]Terminal regime crossover temperature obtained by oscillatory shear rheology during temperature ramp experiments, 2 °C·min^{-1}. [f]Onset of thermal decomposition, as measured by TGA (Figure S27b). [g]Low-temperature glassy plateau modulus obtained by oscillatory shear rheology during temperature ramp experiments, 2 °C·min^{-1} (Figures S31, S33, S35 and S37). [h]Mid frequency rubbery plateau modulus in the TTS master curves (Figures S32, S34, S36, and S38). [i]Entanglement molecular weight, as determined from the plateau modulus, G_N^0, located at the minimum of the tan(δ) curves in the TTS master curves. [j]Terminal relaxation time obtained as $\tau_t = \omega^{-1}$ at which $G' = G''$ in the TTS master curves. [k]Zero shear viscosity, obtained from the low-frequency plateau of the TTS master curves (Figures S32, S34, S36 and S38).

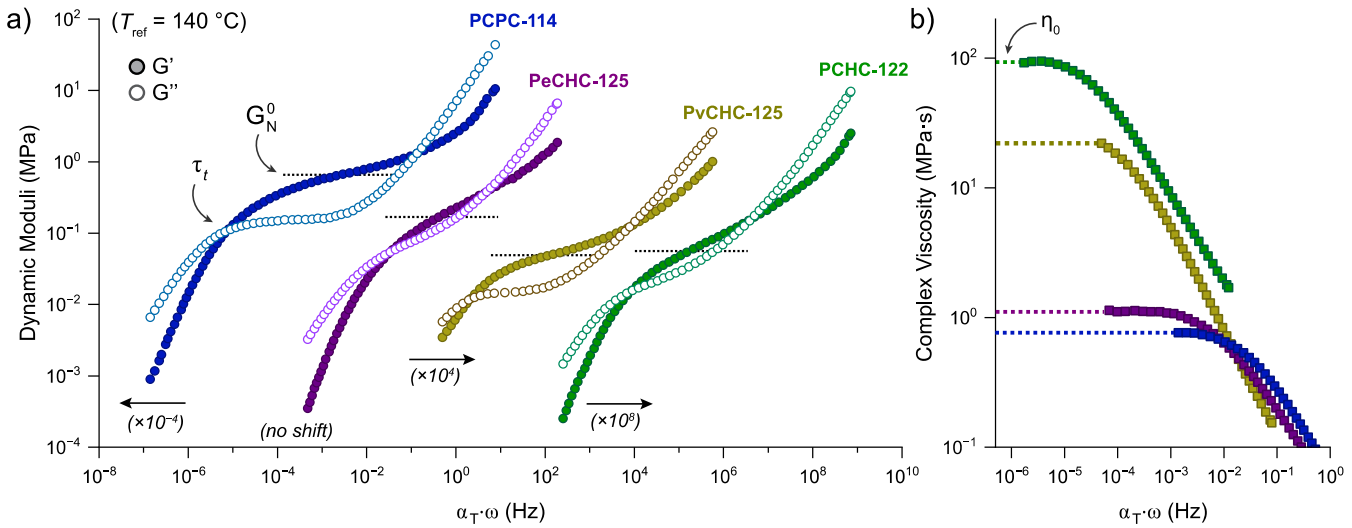

Figure 6. Rheological characterization of high molar mass polycarbonates: PCPC-114 (blue), PeCHC-120 (purple), PvCHC-125 (containing 0.1 wt % of PEHC as the thermal stabilizer, dark yellow), and PCHC-122 (green). (a) Plot of dynamic moduli (G' and G'') vs frequency (Hz), obtained from TTS master curves (curves have been shifted horizontally for clarity, and the shift factors applied to each master curve are specified in the plot; for unshifted TTS master curves see the Supporting Information). (b) Plot of shear viscosity vs frequency (Hz) obtained from TTS master curves and projection of the plateau viscosity to zero-shear.

by differential scanning calorimetry (DSC), thermogravimetric analysis (TGA), and oscillatory shear rheology (Table 3). All the samples are amorphous plastics showing high glass transition temperatures (T_g) with values, as determined by DSC, in the range 85−126 °C, which are dependent on the ring-size and alkyl-substituents (Figure S27a). As such, the T_g for PCHC, featuring the 6-membered ring ($T_{g,DSC}$ = 126 °C, which is at the limit predicted by the Fox−Flory equation),[46] was ∼40 °C higher than for PCPC, which features the 5-membered ring ($T_{g,DSC}$ = 85 °C).[79] Substituted rings show greater segmental motion compared to nonsubstituted ones, i.e., added pendant alkyl chains resulted in a slight reduction of the T_g values. Specifically, PvCHC (vinyl-substituted) and PeCHC (ethyl-substituted) showed T_g values of 118 and 105 °C, respectively, which are 8−25 °C lower than PCHC. As expected, the polymer molar mass influences the glass transition temperature, with values increasing with molar mass, e.g., PvCHC with M_n 16 kg mol^{-1} shows a glass transition temperature of 112 °C, whereas the sample with M_n 82 kg mol^{-1} shows a T_g of 118 °C (Figure S28).

Another method to measure the glass transition temperature is from the peak in tan(δ) obtained during variable temperature oscillatory rheology (Figures S31−S38). Analysis of the samples using this method reveals the same trend of increasing glass transition temperatures depending on the ring sizes and pendent alkyl chains, with values increasing in the order PCPC < PeCHC < PvCHC < PCHC. Compared with those measured by DSC, T_g's determined by rheology are all slightly higher. In addition, all polymers show the necessary high temperature stability, with the onset of thermal decomposition occurring at temperatures (T_d) above 265 °C (Figure S27b). These results indicate a wide processing temperature range, from 135 to 250 °C in all cases. It is noted that the high-temperature stability was dependent upon effective purification to remove residual catalyst, achieved by precipitation and silica-plug filtration (see the Supporting Information for details).

Further insights into the polymers' molecular dynamics and extent of entanglement were obtained from the time and temperature data acquired by oscillatory shear rheology in the melt (Table 2). During temperature ramps (0.5% strain, 1.0 Hz, 2 °C·min^{-1}), all the polycarbonates display four typical viscoelastic regions: a glassy state, a glass transition, a rubbery plateau, and viscous flow, whose characteristic temperatures

https://doi.org/10.1021/jacs.3c14170
J. Am. Chem. Soc. 2024, 146, 8381−8393

and moduli values depend on the backbone ring size and alkyl substituents (Figures S31, S33, S35, and S37). First, only small variations were observed in the high glassy plateau moduli at the start of the oscillatory temperature investigations, with G' ~ 450−460 MPa. Next, the glass transitions are marked by a sharp drop in the viscoelastic moduli and a subsequent peak in the tan(δ), which varied from 97 °C for PCPC to ~130 °C for PvCHC and PCHC. The crossover temperature is the point at which $G' = G''$ and marks the end of the rubbery plateau. These are lowest for PeCHC and PCPC at 161−166 °C and increase to 192−196 °C for PCHC and a stabilized sample of PvCHC (0.1 wt % of a radical inhibitor, pentaerythritol tetrakis (3,5-di-*tert*-butyl-4-hydroxyhydrocinnamate), PEHC).

To further probe the influence of the polymer structure on the molecular dynamics, the samples were analyzed by variable frequency rheology, at constant 10 °C intervals, and the data were used to construct TTS master curves (Figure 6a,b and S32, S34, S36 and S38, reference temperature, T_{ref}, set at 140 °C). In these investigations, PvCHC-125 was stabilized with 0.1 wt % of PEHC to prevent cross-linking (Figure S47). The shift factors, a_T, showed excellent fits to the Williams−Landel−Ferry equation (Table S4 and Figures S39−S46). Similar to the observations in the temperature ramps, all the polycarbonates display typical thermoplastic behavior: their viscoelastic response changes from the glassy state at high frequencies to viscous flow at low frequencies, passing through a rubbery plateau at intermediate frequencies. There are, however, some notable differences in the viscoelastic parameters within the series of materials, signaling the significant influence of the polymer backbone structure on both the slow (long-distance chain entanglements) and fast (short-distance segmental rearrangements, i.e., molecular motions corresponding to the monomer repeat unit) relaxation processes. In the transition zone, both of the dynamic moduli (G' and G'') show a strong frequency dependence. This results in a characteristic maximum in the tan(δ) data, which correlates approximately with the middle of the transition zone. The values for $\tan(\delta)_{max}$ occur at the lowest frequencies for PCHC (4.3 Hz), which is 1 order of magnitude lower than for PeCHC and PvCHC (33−70 Hz) and 4 orders of magnitude lower than for PCPC (42000 Hz). The longer times needed for PCHC suggest that its cyclohexyl groups exert a greater resistance to molecular motions than alkyl-substituted rings and those with one fewer carbon atom. The resistance may arise from conformational effects, for example, the cyclohexene chair conformations may move more slowly through the polymer matrix than other repeat units.[46]

At intermediate relaxation times, the decrease of storage and loss moduli with frequency is less severe, giving rise to a plateau region in G'. In this region, the polymer viscoelastic properties are influenced by chain entanglements that restrain long-range motions. The rubbery plateau modulus, G_N^0, can be determined from the minimum of the tan(δ) in this region, allowing for the estimation of M_e using the tube model equation

$$M_e = \frac{4}{5} \times \frac{\rho RT}{G_N^0}$$

where ρ is the polymer density (see the Supporting Information for estimates), R is the gas constant, and T is the temperature.[80,81] Importantly, the best performing thermoplastics typically show low values of M_e. The comparison of this series of polymers reveals that the cyclohexyl ring polymers, PCHC and PvCHC, both show M_e values that are >10 times higher (~54−56 kg mol^{-1}) than the cyclopentyl ring-substituted polymer, PCPC (M_e ~ 4.0 kg mol^{-1}). Due to the high molar masses and narrow dispersity values of the polymers described in this work, values of M_e obtained for PCHC are 4 times greater than those previously estimated.[45,46] Intriguingly, ethyl-substituted PeCHC displays a somewhat intermediate value of M_e ~ 15 kg mol^{-1} between these two extremes. It is clear from these results that ring-size and alkyl substitution directly influence the molecular dynamics, including the distance between entanglements.

Finally, at shorter frequencies and after modulus crossover, the materials begin to undergo a Newtonian flow. In this region, the relaxation time, τ, of the bulk material is correlated to the crossover frequency where $\tau = 1/\omega$ at the point where $G' = G''$ (Tables 2, and S4). In the series of polymers, PCHC shows the longest relaxation times (4 h) followed by PvCHC (~1.5 h), while PeCHC and PCPC had comparatively fast relaxations (0.2−1 min). In this region, the complex viscosity also reaches a plateau, i.e., the zero shear viscosity, η_0. At the reference temperatures, PCPC and PeCHC show 115× and 70× lower η_0 values than PCHC, another beneficial property for polymer processing.

Films of the polymers (PvCHC-125, PCHC-122, PCPC-114, and PeCHC-125) were prepared for tensile mechanical investigations by solvent casting (from methylene chloride solutions) into Teflon molds, followed by solvent evaporation at ambient temperature for 48 h, and then by heating at 140 °C, under high vacuum, for 24 h. The resulting materials were processed by compression molding above the glass transition temperature (for 10 min and 4 t of pressure) to obtain homogeneous films. GPC analyses of the polymers before and after processing showed identical molar mass and dispersity values, indicating that they remained stable under these conditions (Figures S52−S54). From the films, dumbbell-shaped specimens were cut, according to ISO 527-2 type 5B, and subjected to unilateral extension experiments, conducted according to ISO 527 (Table 3, Figures 7 and S60a). All the polycarbonates are strong plastics with variable tensile strengths, Youngs moduli, and toughness values. High molar mass PCPC-114 is both the strongest and most ductile, with a tensile strength reaching 58.5 ± 1.7 MPa and strain at break of 7.1 ± 1.9%. The PvCHC shows a tensile strength of 52.2 MPa and strain at break ~5%. PCHC is both the weakest and most brittle, with an average tensile strength of 40.0 MPa and a strain at break of ~3%; it also has the highest Young's modulus of 2.2 GPa. The sample containing the ethyl substituent PeCHC shows better properties than the other two six-

Table 3. Mechanical Properties of Selected High Molar Mass Polycarbonates

polymer	σ (MPa)[a]	ε_b (%)[b]	E_y (GPa)[c]	u_t (MJ·m^{-3})[d]
PvCHC-125	52.2 ± 1.0	4.9 ± 1.3	1.33 ± 0.11	1.6 ± 0.6
PCHC-122	40.0 ± 1.8	3.3 ± 0.3	2.16 ± 0.06	0.9 ± 0.1
PCPC-114	58.5 ± 1.7	7.1 ± 1.9	1.70 ± 0.09	2.9 ± 1.1
PeCHC-125	46.7 ± 1.3	18.7 ± 4.2	1.31 ± 0.05	7.0 ± 1.5

[a]Ultimate tensile strength. [b]Strain at break. [c]Young's modulus. [d]Tensile toughness. Mean values ± std. dev. from measurements conducted independently on at least 4 specimens (Figures S55−S58 for full data).

https://doi.org/10.1021/jacs.3c14170
J. Am. Chem. Soc. 2024, 146, 8381−8393

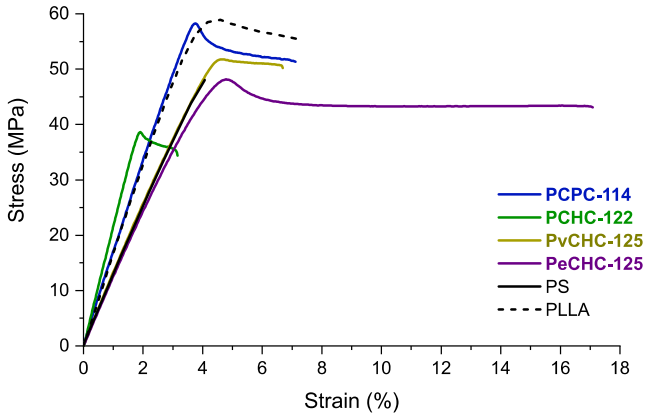

Figure 7. Representative stress vs strain data for high molar mass polycarbonates, dumbbell specimens by ISO 527, test speed of 10 mm·min^{-1} (full data in Figures S55−S58).

membered ring samples, with 5× greater elongation at break (18.7 ± 4.2%) and tensile toughness (46.7 ± 1.3 MPa) compared with PCHC (Table 3, entry 4).

Polycarbonate Recycling. All new polymers should be investigated for efficient end-of-life recycling by both mechanical reprocessing and chemical recycling to monomers. Since these thermoplastics are all amorphous, they should be amenable to reprocessing at temperatures above the T_g. The potential for mechanical recycling was explored by compression molding samples that had been subjected to mechanical testing. Samples of both PCHC-122 and PCPC-114 were reprocessed into homogeneous films and their mechanical properties were tested again (Figure S60b). Both samples showed tensile mechanical profiles equivalent to those of the original samples, indicating the potential for future mechanical recycling of the polymers (Figure S61).

Next, the potential for polycarbonate chemical recycling to the constituent epoxides and carbon dioxide was explored in the solid state with catalyst **1**. Recently, we reported an efficient method for the chemical recycling of neat PCHC films, containing a dispersed catalyst, and investigated depolymerization rates using polymer weight loss vs time at constant temperature by thermogravimetric analysis.[68] Following the same successful film recycling protocol, the polycarbonates were mixed with **1** in the solvent (THF) and cast as films into the TGA crucibles, followed by the complete removal of the solvent (Supporting Information for details). The polymer films were chemically recycled by heating to 140 °C, at a N_2 flow rate of 25 mL min^{-1}, and with continual monitoring of sample weight loss vs time. Using catalyst **1**, at loadings of 1:300, all of the polymers were efficiently depolymerized and formed only the starting *cis*-epoxide and CO_2 as determined by in situ FTIR measurements (Figure 8a, Table S6, Figures S63−S66). It is noteworthy that even though the polymers are atactic, in all cases, depolymerization conversion and selectivity into *cis*-epoxide is high; absolute stereochemistry does not affect depolymerization, only relative *trans*-stereochemistry is important for chain-end backbiting to occur (Figure S67).

In all cases, the recycling occurred quickly, with typical TOF values of 700−1400 h^{-1}. The chemical recycling rates were fastest for the PCPC and decreased in the order PCPC > PvCHC > PeCHC ∼ PCHC. The rate differences are proposed to arise from different stabilities for the alkoxide

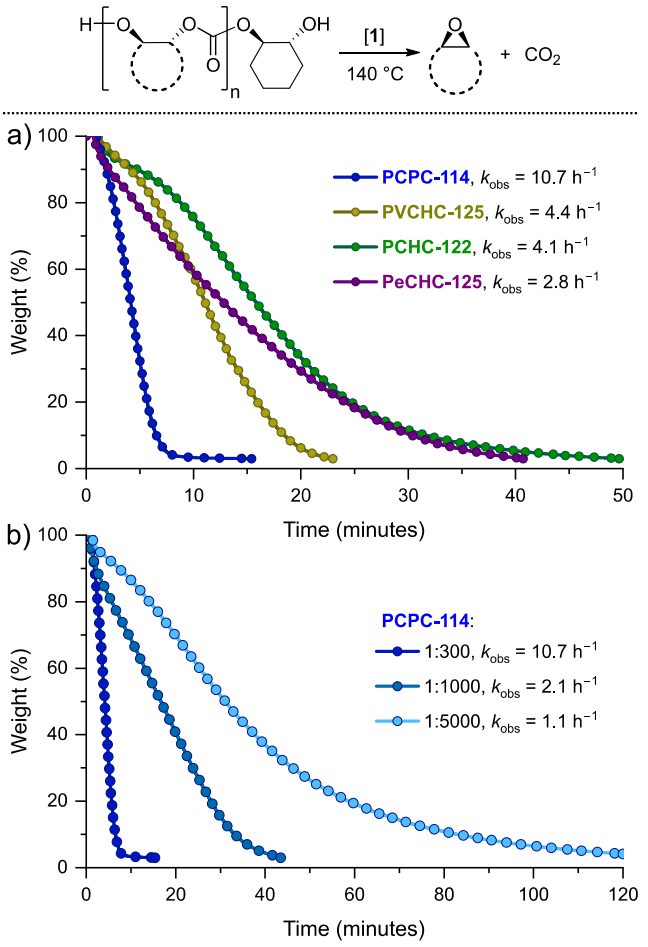

Figure 8. Isothermal TGA data at 140 °C comparing the chemical recycling of the polycarbonates in the presence of catalyst **1**: (a) constant [**1**]:[polycarbonate] (repeat unit) ratio of 1:300. (b) PCPC depolymerization with variable [**1**]:[PCPC] (repeat unit) ratio (Supporting Information for details). The data were fit using exponential functions, which allow for determination of recycling rates.

intermediates and/or from different transition state barriers to epoxide extrusion.[63] Given the fast rates and promising thermal/mechanical properties of PCPC, it was selected for further insights into depolymerization catalysis. As such, progressively lower loadings of the catalyst were explored for the depolymerization reactions (Figure 8b). All depolymerizations were successful, yielding only epoxide (CPO) and CO_2 and could be achieved at catalyst loadings of just 0.02 mol % (1:5000) and with a high TOF value of 2500 h^{-1} (Table S6). Finally, a larger-scale chemical recycling was conducted using ∼2 g of PCPC ([**1**]:[PCPC] 1:1000) in glassware (see the Supporting Information). After 1 h, at 140 °C, the epoxide was isolated in 72% yield and high purity, as indicated by ^{1}H NMR spectroscopy (Figures S68). The depolymerization mechanism was studied for catalyst **2** in our prior work, where we proposed that depolymerization occurs via a chain-end mechanism. It is postulated that catalyst **1** operates by the same mechanism: when acetyl-end-capped PCHC (PCHC-OAc, Figure S69 for end-group analyses) was subjected to depolymerization conditions, no reaction occurred (Figure S70). With PCHC-OAc, hydrolysis of the organometallic catalyst **1** to form the alkoxide intermediate does not occur,

https://doi.org/10.1021/jacs.3c14170
J. Am. Chem. Soc. 2024, 146, 8381−8393

which is a key step in chain-end depolymerization, and hence why no reaction was observed.

It is worth noting that a thermally cross-linked sample of PvCHC also underwent chemical depolymerization to vCHO under isothermal depolymerization at 140 °C in the TGA furnace (see the Supporting Information and Figures S71 and S72) and in the bulk. The low volatility under these conditions of the putative bis-epoxide cross-linker is expected since it was not detected by ^{1}H NMR in the isolated monomer fraction (Figure S73). The 94% weight loss indicated a lightly cross-linked sample, i.e., only containing 6% weight of thermosetting units which, notably, did not impede its efficient depolymerization.

DISCUSSION

This work has established a successful new organometallic catalyst to produce a series of CO_2-based polycarbonates, evaluated their properties, and recommended upon conditions for future reprocessing and depolymerization as a means of manufacture. Moreover, the catalysis advances described herein yield polycarbonates with sufficiently high molar mass values to more accurately determine and compare M_e values. The data are also fully consistent with the difficulties in processing and testing brittle PCHC: almost all prior investigations used samples that were below the critical molar mass or chain entanglement thresholds.[43,45,46,54,56] Certainly, the steep frequency dependence of the G' data in the rubbery plateau region makes the evaluation of M_e still somewhat challenging, and more refined estimates from the value of ∼56 kg mol^{-1} might still be possible in the future. In contrast, the much less widely investigated PCPC shows an order of magnitude lower M_e, with entanglement being of the same magnitude as other strong thermoplastics, e.g., BPA-PC M_e = 1.6−4.8 kg mol^{-1}, and is considerably lower than brittle thermoplastics, e.g., PLLA, M_e = 8−10 kg mol^{-1};[82] PS, M_e = 13−18 kg mol^{-1}.[83] These data all suggest that future applications requiring high tensile strength and toughness should prioritize the five-membered cyclopentene or the ethyl-substituted cyclohexene ring substituents since the optimal thermal-mechanical properties will be accessed at substantially lower molar masses than the six-membered ring analogue.

Our mechanical data on the series of polycarbonates show that the most promising samples, PCPC and PeCHC, show favorable properties, with some in the range of existing commercial thermoplastics (Table S5). For example, PCPC has similar tensile mechanical properties to PLLA but is fully amorphous and shows a significantly higher glass transition temperature than PLLA, which would extend its upper use temperature (PCPC T_g = 85 °C vs PLLA T_g = 50−60 °C, respectively). Further, PCPC can undergo lower energy mechanical recycling than PLLA since the melting temperature for PLLA is typically 160−180 °C, whereas PCPC was effectively mechanically recycled, by compression molding, at 100 °C and displays a η_0 of 0.78 MPa s.[84] It is important to emphasize that, as an added benefit, the high carbonate linkage content in PCPC delivers 34 wt % carbon dioxide utilization (vs 30 wt % for PCHC). To maximize carbon dioxide utilization, the epoxide could also be sourced from biomass; there are already efficient routes to cyclopentene from lignocellulosic biomass since it is proposed for use in biobased aviation fuels.[85] The synthesis involves bioderived furfuraldehyde being hydrogenated, over copper catalysts, to cyclopentanol in 60−90% yield and subsequent alcohol dehydration to cyclopentene, achieved in 84% yield using a recyclable solid acid catalyst.[85,86]

Our investigation also rationalizes the lack of development of PCHC as a stand-alone material—very few catalysts have ever accessed the optimal molar masses for better properties and in any case the high zero shear viscosity (90 MPa s) and moderate tensile mechanical properties suggest it would be best applied within copolymer structures in future.[38,47,48,54] In contrast, PeCHC, featuring an ethyl substituent on the cyclohexene ring, combines high tensile strength (47 MPa), reasonable ductility (19% elongation at break), high glass transition temperatures (105 °C), low entanglement molar mass (13−18 kg mol^{-1}), and low zero shear viscosity (1.26 MPa s). It is recommended for further development as a thermoplastic and may inspire the investigation of other substituted cyclohexane rings. Given that using bioderived epoxides may also help increase carbon dioxide uptake, terpenes such as limonene or menthene also feature substituted cyclohexane rings and their epoxides have precedent in this catalysis.[67,87−91] Limonene oxide is challenging to polymerize due to its tertiary structure,[89,90] but menth-2-ene oxide is an important future target given the influence in this work of ethyl substituents.[92] Greiner and Agarwal reported a route to prepare moderate molar mass poly(meth-2-ene carbonate) (M_n = 20−30 kg mol^{-1}), and the polymer showed a higher glass transition temperature (T_g = 144 °C) and higher temperature stability (T_d = 308 °C) than PCHC.[92] In the future, the organometallic Mg(II)Co(II) catalyst could be used to target molar mass of poly(menth-2-ene carbonate) and determine its entanglement molar mass, tensile mechanical properties, and zero shear viscosity.

In the chemical recycling of polycarbonates to epoxides and carbon dioxide, complex **1** combines high rates, outstanding selectivity, and low loading tolerance and operates effectively using high molar mass polycarbonate—it is fastest using PCPC. Compared with other efficient PCPC depolymerization catalysts and processes its performance is excellent (Table S6). For example, catalyst **1** compares favorably against one of the best catalysts yet reported for PCPC recycling (Figure S62 for catalyst structures).[48] The ammonium diborane catalyst is highly effective but requires the addition of KOH for activity. Even so, catalyst **1** enables depolymerization at 100× lower loading and shows ∼2000× higher activity. **1** is also more active than [Cr(salen)(Cl)]/PPN(N_3) catalyst system which operates in neat polymer, showing efficient depolymerization at 60 °C lower temperature, using 10× lower loading and at ∼4× higher activity.[65] Complex **1** also surpasses the original [Cr(salen)(Cl)]/^{n}Bu$_4$NN_3 catalyst, used in solution in Darensbourg and co-workers' seminal work, achieving activity values that are ∼2500× higher and operating at 1/100 loading.[61] These data also support future focus on PCPC since it shows the most efficient chemical recycling catalysis and allowed, in laboratory scale experiments, for efficient closed loop recycling to cyclopentene oxide and CO_2.

CONCLUSIONS

A new organometallic Mg(II)Co(II) catalyst, applied with a diol, showed outstanding productivity and initiation control in the ROCOP of CO_2 and cyclic epoxides. It was used to make a series of high molar mass polycarbonates, with M_n from 100 to 163 kg mol^{-1}, by copolymerization of CO_2 with vCHO, CHO, or CPO. The physical properties of these carbon dioxide-thermoplastics, together with an ethyl-substituted eCHO

https://doi.org/10.1021/jacs.3c14170
J. Am. Chem. Soc. 2024, 146, 8381−8393

derived by hydrogenation of vinyl-polycarbonate, were investigated. The thermal, mechanical, and rheological experiments all demonstrate the significant influence of the ring size and alkyl-substituents over properties. The most widely investigated material in the literature, PCHC, showed a high temperature glass transition but suffered with low tensile strength and brittleness due to a lack of chain entanglements. Its entanglement molecular weight, M_e, was very high (56 kg mol^{-1}), which complicates future processing and applications. Achieving optimal properties will require ultrahigh molar mass samples (>10^3 kg mol^{-1}),[93−96] with concomitant processing limitations due to its high viscosity. As such, perhaps it will be better to limit the use of PCHC as a stand-alone material and investigate its beneficial properties within copolymer structures. On the other hand, exactly the opposite conclusion is made regarding PCPC, which shows significant potential as a future thermoplastic. A PCPC with M_n = 114 kg mol^{-1} showed high tensile strength (59 MPa), high Young's modulus (1.7 GPa), moderate elongation at break (7%), high tensile toughness (3 MJ m^{-3}), a medium/high glass transition temperature (T_g = 85 or 97 °C by DSC or rheology), and low zero shear viscosity (0.78 MPa s). These properties arise from its low M_e (∼4 kg mol^{-1}) with the consequence that in the future, only moderate molar mass polymers should be required to achieve the best material properties. Its properties are similar to those of polystyrene, albeit with a lower M_e, and it improves upon the high use temperature limitations of poly(L-lactide) (PLLA). All the polycarbonates, including PCPC, are fully reprocessable by compression molding (100−140 °C, 10 min), providing a future mechanical recycling route. Further, the new Mg(II)Co(II) catalyst efficiently depolymerized the high molar mass polycarbonates to epoxides and CO_2, providing a future chemical recycling option. The lead material, PCPC, underwent the fastest depolymerizations with high activity (TOF = 2500 h^{-1}) and low catalyst loadings (1:5000), exceeding performances by several orders of magnitude for current literature catalysts. In future, PCPC should be prioritized for further investigation both in catalysis, application development and recycling chemistry. The new organometallic Mg(II)Co(II) catalyst, with its high productivity, low loading, and efficiency in either CO_2 polymerization or depolymerization, should be investigated using other monomers and polymerizations to diversify the range of CO_2-based polymers.

■ ASSOCIATED CONTENT

Supporting Information

The Supporting Information is available free of charge at https://pubs.acs.org/doi/10.1021/jacs.3c14170.

Characterization data of complexes (NMR, X-ray crystallography, magnetic moment, CV); polymerization data (NMR, MALDI-ToF, GPC chromatograms, DSC, TGA, Rheology, Tensile Testing); chemical recycling data (NMR, TGA-FTIR); and CheckCIF/PLATON report (PDF)

Accession Codes

CCDC 2208898 and 2208899 contain the supplementary crystallographic data for this paper. These data can be obtained free of charge via www.ccdc.cam.ac.uk/data_request/cif, or by emailing data_request@ccdc.cam.ac.uk, or by contacting The Cambridge Crystallographic Data Centre, 12 Union Road, Cambridge CB2 1EZ, UK; fax: +44 1223 336033.

■ AUTHOR INFORMATION

Corresponding Author

Charlotte K. Williams − *Department of Chemistry, Chemistry Research Laboratory, University of Oxford, Oxford OX1 3TA, U.K.;* orcid.org/0000-0002-0734-1575; Email: charlotte.williams@chem.ox.ac.uk

Authors

Gloria Rosetto − *Department of Chemistry, Chemistry Research Laboratory, University of Oxford, Oxford OX1 3TA, U.K.;* Present Address: Renewable Resources and Enabling Sciences Center, National Renewable Energy Laboratory, Golden, CO 80401, United States; orcid.org/0009-0009-7116-7258

Fernando Vidal − *Department of Chemistry, Chemistry Research Laboratory, University of Oxford, Oxford OX1 3TA, U.K.;* Present Address: POLYMAT, University of the Basque Country UPV/EHU, Joxe Mari Korta Center, Avda. Tolosa 72, 20018 Donostia-San Sebastian, Spain; orcid.org/0000-0002-3027-768X

Thomas M. McGuire − *Department of Chemistry, Chemistry Research Laboratory, University of Oxford, Oxford OX1 3TA, U.K.;* orcid.org/0000-0002-2719-1228

Ryan W. F. Kerr − *Department of Chemistry, Chemistry Research Laboratory, University of Oxford, Oxford OX1 3TA, U.K.;* orcid.org/0000-0002-8045-2060

Complete contact information is available at: https://pubs.acs.org/10.1021/jacs.3c14170

Notes

The authors declare the following competing financial interest(s): C.K.W. is a director of Econic Technologies Ltd.

■ ACKNOWLEDGMENTS

The Engineering and Physical Sciences Research Council (EPSRC, EP/S018603/; EP/R027129/1), the UK Catalysis Hub (EP/R027129/1), Research England (iCAST, RED, RE-P-2020-04), The Oxford Martin School (Future of Plastics), and the EU Horizon Programme (Marie Skłodowska-Curie no. 101018516) are acknowledged for research funding.

■ REFERENCES

(1) Bachmann, M.; Zibunas, C.; Hartmann, J.; Tulus, V.; Suh, S.; Guillén-Gosálbez, G.; Bardow, A. Towards circular plastics within planetary boundaries. *Nat. Sustain.* **2023**, *6* (5), 599−610.

(2) Zheng, J.; Suh, S. Strategies to reduce the global carbon footprint of plastics. *Nat. Clim. Change* **2019**, *9* (5), 374−378.

(3) Nicholson, S. R.; Rorrer, N. A.; Carpenter, A. C.; Beckham, G. T. Manufacturing energy and greenhouse gas emissions associated with plastics consumption. *Joule* **2021**, *5* (3), 673−686.

(4) Jehanno, C.; Alty, J. W.; Roosen, M.; De Meester, S.; Dove, A. P.; Chen, E. Y. X.; Leibfarth, F. A.; Sardon, H. Critical advances and future opportunities in upcycling commodity polymers. *Nature* **2022**, *603* (7903), 803−814.

(5) Haque, F. M.; Ishibashi, J. S. A.; Lidston, C. A. L.; Shao, H.; Bates, F. S.; Chang, A. B.; Coates, G. W.; Cramer, C. J.; Dauenhauer, P. J.; Dichtel, W. R.; Ellison, C. J.; Gormong, E. A.; Hamachi, L. S.; Hoye, T. R.; Jin, M.; Kalow, J. A.; Kim, H. J.; Kumar, G.; LaSalle, C. J.; Liffland, S.; Lipinski, B. M.; Pang, Y.; Parveen, R.; Peng, X.; Popowski, Y.; Prebihalo, E. A.; Reddi, Y.; Reineke, T. M.; Sheppard, D. T.; Swartz, J. L.; Tolman, W. B.; Vlaisavljevich, B.; Wissinger, J.; Xu, S.; Hillmyer, M. A. Defining the Macromolecules of Tomorrow through Synergistic Sustainable Polymer Research. *Chem. Rev.* **2022**, *122* (6), 6322−6373.

(6) Stegmann, P.; Daioglou, V.; Londo, M.; van Vuuren, D. P.; Junginger, M. Plastic futures and their CO_2 emissions. *Nature* **2022**, *612* (7939), 272−276.
(7) Coates, G. W.; Getzler, Y. D. Y. L. Chemical recycling to monomer for an ideal, circular polymer economy. *Nat. Rev. Mater.* **2020**, *5* (7), 501−516.
(8) Hong, M.; Chen, E. Y. X. Completely recyclable biopolymers with linear and cyclic topologies via ring-opening polymerization of γ-butyrolactone. *Nat. Chem.* **2016**, *8* (1), 42−49.
(9) Zhang, X.; Fevre, M.; Jones, G. O.; Waymouth, R. M. Catalysis as an Enabling Science for Sustainable Polymers. *Chem. Rev.* **2018**, *118* (2), 839−885.
(10) Schneiderman, D. K.; Hillmyer, M. A. 50th Anniversary Perspective: There Is a Great Future in Sustainable Polymers. *Macromolecules* **2017**, *50* (10), 3733−3749.
(11) Hepburn, C.; Adlen, E.; Beddington, J.; Carter, E. A.; Fuss, S.; Mac Dowell, N.; Minx, J. C.; Smith, P.; Williams, C. K. The technological and economic prospects for CO_2 utilization and removal. *Nature* **2019**, *575* (7781), 87−97.
(12) Bhat, G. A.; Darensbourg, D. J. Progress in the catalytic reactions of CO_2 and epoxides to selectively provide cyclic or polymeric carbonates. *Green Chem.* **2022**, *24* (13), 5007−5034.
(13) Grignard, B.; Gennen, S.; Jérôme, C.; Kleij, A. W.; Detrembleur, C. Advances in the use of CO_2 as a renewable feedstock for the synthesis of polymers. *Chem. Soc. Rev.* **2019**, *48* (16), 4466−4514.
(14) Lee, S. H.; Cyriac, A.; Jeon, J. Y.; Lee, B. Y. Preparation of thermoplastic polyurethanes using in situ generated poly(propylene carbonate)-diols. *Polym. Chem.* **2012**, *3* (5), 1215−1220.
(15) Schüttner, S.; Gardiner, C.; Petrov, F. S.; Fotaras, N.; Preis, J.; Floudas, G.; Frey, H. Biobased Thermoplastic Elastomers Derived from Citronellyl Glycidyl Ether, CO_2, and Polylactide. *Macromolecules* **2023**, *56* (20), 8247−8259.
(16) Scharfenberg, M.; Hofmann, S.; Preis, J.; Hilf, J.; Frey, H. Rigid Hyperbranched Polycarbonate Polyols from CO_2 and Cyclohexene-Based Epoxides. *Macromolecules* **2017**, *50* (16), 6088−6097.
(17) Scharfenberg, M.; Hilf, J.; Frey, H. Functional Polycarbonates from Carbon Dioxide and Tailored Epoxide Monomers: Degradable Materials and Their Application Potential. *Adv. Funct. Mater.* **2018**, *28* (10), 1704302.
(18) Yang, G.-W.; Wu, G.-P. High-Efficiency Construction of CO_2-Based Healable Thermoplastic Elastomers via a Tandem Synthetic Strategy. *ACS Sustain. Chem. Eng.* **2019**, *7* (1), 1372−1380.
(19) Cao, H.; Zhang, R.; Zhou, Z.; Liu, S.; Tao, Y.; Wang, F.; Wang, X. On-Demand Transformation of Carbon Dioxide into Polymers Enabled by a Comb-Shaped Metallic Oligomer Catalyst. *ACS Catal.* **2022**, *12* (1), 481−490.
(20) Deng, J.; Ratanasak, M.; Sako, Y.; Tokuda, H.; Maeda, C.; Hasegawa, J.-y.; Nozaki, K.; Ema, T. Aluminum porphyrins with quaternary ammonium halides as catalysts for copolymerization of cyclohexene oxide and CO_2: metal-ligand cooperative catalysis. *Chem. Sci.* **2020**, *11* (22), 5669−5675.
(21) Kember, M. R.; Knight, P. D.; Reung, P. T. R.; Williams, C. K. Highly Active Dizinc Catalyst for the Copolymerization of Carbon Dioxide and Cyclohexene Oxide at One Atmosphere Pressure. *Angew. Chem., Int. Ed.* **2009**, *48* (5), 931−933.
(22) Rosetto, G.; Deacy, A. C.; Williams, C. K. Mg(ii) heterodinuclear catalysts delivering carbon dioxide derived multi-block polymers. *Chem. Sci.* **2021**, *12* (37), 12315−12325.
(23) Nagae, H.; Aoki, R.; Akutagawa, S.-n.; Kleemann, J.; Tagawa, R.; Schindler, T.; Choi, G.; Spaniol, T. P.; Tsurugi, H.; Okuda, J.; Mashima, K. Lanthanide Complexes Supported by a Trizinc Crown Ether as Catalysts for Alternating Copolymerization of Epoxide and CO_2: Telomerization Controlled by Carboxylate Anions. *Angew. Chem., Int. Ed.* **2018**, *57* (9), 2492−2496.
(24) Deacy, A. C.; Phanopoulos, A.; Lindeboom, W.; Buchard, A.; Williams, C. K. Insights into the Mechanism of Carbon Dioxide and Propylene Oxide Ring-Opening Copolymerization Using a Co(III)/K(I) Heterodinuclear Catalyst. *J. Am. Chem. Soc.* **2022**, *144* (39), 17929−17938.
(25) Lindeboom, W.; Deacy, A. C.; Phanopoulos, A.; Buchard, A.; Williams, C. K. Correlating Metal Redox Potentials to Co(III)K(I) Catalyst Performances in Carbon Dioxide and Propene Oxide Ring Opening Copolymerization. *Angew. Chem., Int. Ed.* **2023**, *62* (37), No. e202308378.
(26) Diment, W. T.; Lindeboom, W.; Fiorentini, F.; Deacy, A. C.; Williams, C. K. Synergic Heterodinuclear Catalysts for the Ring-Opening Copolymerization (ROCOP) of Epoxides, Carbon Dioxide, and Anhydrides. *Acc. Chem. Res.* **2022**, *55* (15), 1997−2010.
(27) Deacy, A. C.; Kilpatrick, A. F. R.; Regoutz, A.; Williams, C. K. Understanding metal synergy in heterodinuclear catalysts for the copolymerization of CO_2 and epoxides. *Nat. Chem.* **2020**, *12* (4), 372−380.
(28) Cheng, M.; Lobkovsky, E. B.; Coates, G. W. Catalytic Reactions Involving C1 Feedstocks: New High-Activity Zn(II)-Based Catalysts for the Alternating Copolymerization of Carbon Dioxide and Epoxides. *J. Am. Chem. Soc.* **1998**, *120* (42), 11018−11019.
(29) Lehenmeier, M. W.; Kissling, S.; Altenbuchner, P. T.; Bruckmeier, C.; Deglmann, P.; Brym, A.-K.; Rieger, B. Flexibly Tethered Dinuclear Zinc Complexes: A Solution to the Entropy Problem in CO_2/Epoxide Copolymerization Catalysis? *Angew. Chem., Int. Ed.* **2013**, *52* (37), 9821−9826.
(30) Liu, Y.; Ren, W.-M.; Liu, J.; Lu, X.-B. Asymmetric Copolymerization of CO_2 with meso-Epoxides Mediated by Dinuclear Cobalt(III) Complexes: Unprecedented Enantioselectivity and Activity. *Angew. Chem., Int. Ed.* **2013**, *52* (44), 11594−11598.
(31) Asaba, H.; Iwasaki, T.; Hatazawa, M.; Deng, J.; Nagae, H.; Mashima, K.; Nozaki, K. Alternating Copolymerization of CO_2 and Cyclohexene Oxide Catalyzed by Cobalt-Lanthanide Mixed Multinuclear Complexes. *Inorg. Chem.* **2020**, *59* (12), 7928−7933.
(32) Yang, G.-W.; Zhang, Y.-Y.; Xie, R.; Wu, G.-P. Scalable Bifunctional Organoboron Catalysts for Copolymerization of CO_2 and Epoxides with Unprecedented Efficiency. *J. Am. Chem. Soc.* **2020**, *142* (28), 12245−12255.
(33) Taherimehr, M.; Al-Amsyar, S. M.; Whiteoak, C. J.; Kleij, A. W.; Pescarmona, P. P. High activity and switchable selectivity in the synthesis of cyclic and polymeric cyclohexene carbonates with iron amino triphenolate catalysts. *Green Chem.* **2013**, *15* (11), 3083−3090.
(34) Darensbourg, D. J.; Mackiewicz, R. M.; Rodgers, J. L.; Phelps, A. L. (Salen)CrIIIX Catalysts for the Copolymerization of Carbon Dioxide and Epoxides: Role of the Initiator and Cocatalyst. *Inorg. Chem.* **2004**, *43* (6), 1831−1833.
(35) Schütze, M.; Dechert, S.; Meyer, F. Highly Active and Readily Accessible Proline-Based Dizinc Catalyst for CO_2/Epoxide Copolymerization. *Chem.—Eur. J.* **2017**, *23* (65), 16472−16475.
(36) Lee, B. Y.; Kwon, H. Y.; Lee, S. Y.; Na, S. J.; Han, S.-i.; Yun, H.; Lee, H.; Park, Y.-W. Bimetallic Anilido-Aldimine Zinc Complexes for Epoxide/CO_2 Copolymerization. *J. Am. Chem. Soc.* **2005**, *127* (9), 3031−3037.
(37) Zhang, D.; Boopathi, S. K.; Hadjichristidis, N.; Gnanou, Y.; Feng, X. Metal-Free Alternating Copolymerization of CO_2 with Epoxides: Fulfilling "Green" Synthesis and Activity. *J. Am. Chem. Soc.* **2016**, *138* (35), 11117−11120.
(38) Zhang, J.; Wang, L.; Liu, S.; Li, Z. Synthesis of Diverse Polycarbonates by Organocatalytic Copolymerization of CO_2 and Epoxides: From High Pressure and Temperature to Ambient Conditions. *Angew. Chem., Int. Ed.* **2022**, *61* (4), No. e202111197.
(39) Kozak, C. M.; Ambrose, K.; Anderson, T. S. Copolymerization of carbon dioxide and epoxides by metal coordination complexes. *Coord. Chem. Rev.* **2018**, *376*, 565−587.
(40) Chen, C.; Gnanou, Y.; Feng, X. Ultra-Productive Upcycling CO_2 into Polycarbonate Polyols via Borinane-Based Bifunctional Organocatalysts. *Macromolecules* **2023**, *56* (3), 892−898.
(41) Schaefer, J.; Zhou, H.; Lee, E.; Lambic, N. S.; Culcu, G.; Holtcamp, M. W.; Rix, F. C.; Lin, T.-P. Tertiary and Quaternary Phosphonium Borane Bifunctional Catalysts for CO_2/Epoxide

https://doi.org/10.1021/jacs.3c14170
J. Am. Chem. Soc. 2024, 146, 8381−8393

Copolymerization: A Mechanistic Investigation Using In Situ Raman Spectroscopy. *ACS Catal.* **2022**, *12* (19), 11870−11885.
(42) Darensbourg, D. J. Chain transfer agents utilized in epoxide and CO_2 copolymerization processes. *Green Chem.* **2019**, *21* (9), 2214−2223.
(43) Sulley, G. S.; Gregory, G. L.; Chen, T. T. D.; Peña Carrodeguas, L.; Trott, G.; Santmarti, A.; Lee, K.-Y.; Terrill, N. J.; Williams, C. K. Switchable Catalysis Improves the Properties of CO_2-Derived Polymers: Poly(cyclohexene carbonate-b-ε-decalactone-b-cyclohexene carbonate) Adhesives, Elastomers, and Toughened Plastics. *J. Am. Chem. Soc.* **2020**, *142* (9), 4367−4378.
(44) Jutz, F.; Buchard, A.; Kember, M. R.; Fredriksen, S. B.; Williams, C. K. Mechanistic Investigation and Reaction Kinetics of the Low-Pressure Copolymerization of Cyclohexene Oxide and Carbon Dioxide Catalyzed by a Dizinc Complex. *J. Am. Chem. Soc.* **2011**, *133* (43), 17395−17405.
(45) Koning, C.; Wildeson, J.; Parton, R.; Plum, B.; Steeman, P.; Darensbourg, D. J. Synthesis and physical characterization of poly(cyclohexane carbonate), synthesized from CO_2 and cyclohexene oxide. *Polymer* **2001**, *42* (9), 3995−4004.
(46) Spyridakou, M.; Gardiner, C.; Papamokos, G.; Frey, H.; Floudas, G. Dynamics of Poly(cyclohexene carbonate) as a Function of Molar Mass. *ACS Appl. Polym. Mater.* **2022**, *4* (5), 3833−3843.
(47) Jia, M.; Hadjichristidis, N.; Gnanou, Y.; Feng, X. Monomodal Ultrahigh-Molar-Mass Polycarbonate Homopolymers and Diblock Copolymers by Anionic Copolymerization of Epoxides with CO_2. *ACS Macro Lett.* **2019**, *8* (12), 1594−1598.
(48) Yang, G.-W.; Wang, Y.; Qi, H.; Zhang, Y.-Y.; Zhu, X.-F.; Lu, C.; Yang, L.; Wu, G.-P. Highly Selective Preparation and Depolymerization of Chemically Recyclable Poly(cyclopentene carbonate) Enabled by Organoboron Catalysts. *Angew. Chem., Int. Ed.* **2022**, *61* (46), No. e202210243.
(49) Ren, W.-M.; Zhang, X.; Liu, Y.; Li, J.-F.; Wang, H.; Lu, X.-B. Highly Active, Bifunctional Co(III)-Salen Catalyst for Alternating Copolymerization of CO_2 with Cyclohexene Oxide and Terpolymerization with Aliphatic Epoxides. *Macromolecules* **2010**, *43* (3), 1396−1402.
(50) Kong, D.-C.; Yang, M.-H.; Zhang, X.-S.; Du, Z.-C.; Fu, Q.; Gao, X.-Q.; Gong, J.-W. Control of Polymer Properties by Entanglement: A Review. *Macromol. Mater. Eng.* **2021**, *306* (12), 2100536.
(51) Jia, M.; Zhang, D.; de Kort, G. W.; Wilsens, C. H. R. M.; Rastogi, S.; Hadjichristidis, N.; Gnanou, Y.; Feng, X. All-Polycarbonate Thermoplastic Elastomers Based on Triblock Copolymers Derived from Triethylborane-Mediated Sequential Copolymerization of CO_2 with Various Epoxides. *Macromolecules* **2020**, *53* (13), 5297−5307.
(52) Neumann, S.; Däbritz, S. B.; Fritze, S. E.; Leitner, L.-C.; Anand, A.; Greiner, A.; Agarwal, S. Sustainable block copolymers of poly(limonene carbonate). *Polym. Chem.* **2021**, *12* (6), 903−910.
(53) Liu, J.; Jia, M.; Gnanou, Y.; Feng, X. One-Pot Synthesis of CO_2-Based Polylactide-b-Poly(ether carbonate)-b-Polylactide Triblock Copolymers and Their Mechanical Properties. *Macromolecules* **2023**, *56* (4), 1615−1624.
(54) Kernbichl, S.; Rieger, B. Aliphatic polycarbonates derived from epoxides and CO_2: A comparative study of poly(cyclohexene carbonate) and poly(limonene carbonate). *Polymer* **2020**, *205*, 122667.
(55) Hauenstein, O.; Reiter, M.; Agarwal, S.; Rieger, B.; Greiner, A. Bio-based polycarbonate from limonene oxide and CO_2 with high molecular weight, excellent thermal resistance, hardness and transparency. *Green Chem.* **2016**, *18* (3), 760−770.
(56) Bailer, J.; Feth, S.; Bretschneider, F.; Rosenfeldt, S.; Drechsler, M.; Abetz, V.; Schmalz, H.; Greiner, A. Synthesis and self-assembly of biobased poly(limonene carbonate)-block-poly(cyclohexene carbonate) diblock copolymers prepared by sequential ring-opening copolymerization. *Green Chem.* **2019**, *21* (9), 2266−2272.
(57) Romain, C.; Garden, J. A.; Trott, G.; Buchard, A.; White, A. J. P.; Williams, C. K. Di-Zinc-Aryl Complexes: CO_2 Insertions and Applications in Polymerisation Catalysis. *Chem.—Eur. J.* **2017**, *23* (30), 7367−7376.
(58) Diment, W. T.; Williams, C. K. Chain end-group selectivity using an organometallic Al(iii)/K(i) ring-opening copolymerization catalyst delivers high molar mass, monodisperse polyesters. *Chem. Sci.* **2022**, *13* (29), 8543−8549.
(59) Liu, Y.; Lu, X.-B. Emerging Trends in Closed-Loop Recycling Polymers: Monomer Design and Catalytic Bulk Depolymerization. *Chem.—Eur. J.* **2023**, *29* (23), No. e202203635.
(60) Liu, Y.; Lu, X.-B. Chemical recycling to monomers: Industrial Bisphenol-A-Polycarbonates to novel aliphatic polycarbonate materials. *J. Polym. Sci.* **2022**, *60* (24), 3256−3268.
(61) Darensbourg, D. J.; Wei, S.-H.; Yeung, A. D.; Ellis, W. C. An Efficient Method of Depolymerization of Poly(cyclopentene carbonate) to Its Comonomers: Cyclopentene Oxide and Carbon Dioxide. *Macromolecules* **2013**, *46* (15), 5850−5855.
(62) Liu, Y.; Zhou, H.; Guo, J.-Z.; Ren, W.-M.; Lu, X.-B. Completely Recyclable Monomers and Polycarbonate: Approach to Sustainable Polymers. *Angew. Chem., Int. Ed.* **2017**, *56* (17), 4862−4866.
(63) Singer, F. N.; Deacy, A. C.; McGuire, T. M.; Williams, C. K.; Buchard, A. Chemical Recycling of Poly(Cyclohexene Carbonate) Using a Di-MgII Catalyst. *Angew. Chem., Int. Ed.* **2022**, *61* (26), No. e202201785.
(64) Liao, X.; Cui, F.-C.; He, J.-H.; Ren, W.-M.; Lu, X.-B.; Zhang, Y.-T. A sustainable approach for the synthesis of recyclable cyclic CO_2-based polycarbonates. *Chem. Sci.* **2022**, *13* (21), 6283−6290.
(65) Yu, Y.; Gao, B.; Liu, Y.; Lu, X.-B. Efficient and Selective Chemical Recycling of CO_2-Based Alicyclic Polycarbonates via Catalytic Pyrolysis. *Angew. Chem., Int. Ed.* **2022**, *61* (34), No. e202204492.
(66) Yu, Y.; Fang, L.-M.; Liu, Y.; Lu, X.-B. Chemical Synthesis of CO_2-Based Polymers with Enhanced Thermal Stability and Unexpected Recyclability from Biosourced Monomers. *ACS Catal.* **2021**, *11* (13), 8349−8357.
(67) Carrodeguas, L. P.; Chen, T. T. D.; Gregory, G. L.; Sulley, G. S.; Williams, C. K. High elasticity, chemically recyclable, thermoplastics from bio-based monomers: carbon dioxide, limonene oxide and ε-decalactone. *Green Chem.* **2020**, *22* (23), 8298−8307.
(68) McGuire, T. M.; Deacy, A. C.; Buchard, A.; Williams, C. K. Solid-State Chemical Recycling of Polycarbonates to Epoxides and Carbon Dioxide Using a Heterodinuclear Mg(II)Co(II) Catalyst. *J. Am. Chem. Soc.* **2022**, *144* (40), 18444−18449.
(69) Royo, P.; Vazquez, A. Pentafluorophenylcobalt(II) complexes. *J. Organomet. Chem.* **1981**, *204* (2), 243−247.
(70) Smith, C. F.; Tamborski, C. Synthesis and reactions of a bis(pentafluorophenyl)cobalt complex. *J. Organomet. Chem.* **1971**, *32* (2), 257−262.
(71) Rossi, A. R.; Hoffmann, R. Transition metal pentacoordination. *Inorg. Chem.* **1975**, *14* (2), 365−374.
(72) Cheng, M.; Darling, N. A.; Lobkovsky, E. B.; Coates, G. W. Enantiomerically-enriched organic reagents via polymer synthesis: enantioselective copolymerization of cycloalkene oxides and CO_2 using homogeneous, zinc-based catalysts. *Chem. Commun.* **2000**, 2007−2008.
(73) Hilf, J.; Frey, H. Propargyl-Functional Aliphatic Polycarbonate Obtained from Carbon Dioxide and Glycidyl Propargyl Ether. *Macromol. Rapid Commun.* **2013**, *34* (17), 1395−1400.
(74) Zhang, J.-F.; Ren, W.-M.; Sun, X.-K.; Meng, Y.; Du, B.-Y.; Zhang, X.-H. Fully Degradable and Well-Defined Brush Copolymers from Combination of Living CO2/Epoxide Copolymerization, Thiol-Ene Click Reaction and ROP of ε-caprolactone. *Macromolecules* **2011**, *44* (24), 9882−9886.
(75) Darensbourg, D. J.; Tsai, F.-T. Postpolymerization Functionalization of Copolymers Produced from Carbon Dioxide and 2-Vinyloxirane: Amphiphilic/Water-Soluble CO_2-Based Polycarbonates. *Macromolecules* **2014**, *47* (12), 3806−3813.
(76) Yi, N.; Chen, T. T. D.; Unruangsri, J.; Zhu, Y.; Williams, C. K. Orthogonal functionalization of alternating polyesters: selective patterning of (AB)n sequences. *Chem. Sci.* **2019**, *10* (43), 9974−9980.

https://doi.org/10.1021/jacs.3c14170
J. Am. Chem. Soc. 2024, 146, 8381−8393

(77) Plajer, A. J.; Williams, C. K. Heterocycle/Heteroallene Ring-Opening Copolymerization: Selective Catalysis Delivering Alternating Copolymers. *Angew. Chem., Int. Ed.* **2022**, *61*, No. e202104495.
(78) Hillmyer, M. A.; Laredo, W. R.; Grubbs, R. H. Ring-Opening Metathesis Polymerization of Functionalized Cyclooctenes by a Ruthenium-Based Metathesis Catalyst. *Macromolecules* **1995**, *28* (18), 6311−6316.
(79) Darensbourg, D. J.; Chung, W.-C.; Wilson, S. J. Catalytic Coupling of Cyclopentene Oxide and CO_2 Utilizing Bifunctional (salen)Co(III) and (salen)Cr(III) Catalysts: Comparative Processes Involving Binary (salen)Cr(III) Analogs. *ACS Catal.* **2013**, *3* (12), 3050−3057.
(80) Fetters, L. J.; Lohse, D. J.; Richter, D.; Witten, T. A.; Zirkel, A. Connection between Polymer Molecular Weight, Density, Chain Dimensions, and Melt Viscoelastic Properties. *Macromolecules* **1994**, *27* (17), 4639−4647.
(81) Graessley, W. W.; Edwards, S. F. Entanglement interactions in polymers and the chain contour concentration. *Polymer* **1981**, *22* (10), 1329−1334.
(82) Grijpma, D. W.; Penning, J. P.; Pennings, A. J. Chain entanglement, mechanical properties and drawability of poly(lactide). *Colloid Polym. Sci.* **1994**, *272* (9), 1068−1081.
(83) Pawlak, A. The Entanglements of Macromolecules and Their Influence on the Properties of Polymers. *Macromol. Chem. Phys.* **2019**, *220* (10), 1900043.
(84) Farah, S.; Anderson, D. G.; Langer, R. Physical and mechanical properties of PLA, and their functions in widespread applications — A comprehensive review. *Adv. Drug Delivery Rev.* **2016**, *107*, 367−392.
(85) Kang, Q.; Zhang, X.; Cui, Y.; Zhao, X.; Wang, W.; Zhang, J.; Zhang, Q.; Ma, L. Synthesis of high-density bio-jet fuel by one-pot Mannich-Michael reaction and subsequent hydrodeoxygenation over alkali-treated zeolite catalysts. *Fuel* **2023**, *349*, 128706.
(86) Li, X.-L.; Deng, J.; Shi, J.; Pan, T.; Yu, C.-G.; Xu, H.-J.; Fu, Y. Selective conversion of furfural to cyclopentanone or cyclopentanol using different preparation methods of Cu-Co catalysts. *Green Chem.* **2015**, *17* (2), 1038−1046.
(87) Neumann, S.; Leitner, L.-C.; Schmalz, H.; Agarwal, S.; Greiner, A. Unlocking the Processability and Recyclability of Biobased Poly(limonene carbonate). *ACS Sustain. Chem. Eng.* **2020**, *8* (16), 6442−6448.
(88) Li, C.; van Berkel, S.; Sablong, R. J.; Koning, C. E. Post-functionalization of fully biobased poly(limonene carbonate)s: Synthesis, characterization and coating evaluation. *Eur. Polym. J.* **2016**, *85*, 466−477.
(89) Peña Carrodeguas, L.; González-Fabra, J.; Castro-Gómez, F.; Bo, C.; Kleij, A. W. AlIII-Catalysed Formation of Poly(limonene)-carbonate: DFT Analysis of the Origin of Stereoregularity. *Chem.—Eur. J.* **2015**, *21* (16), 6115−6122.
(90) Byrne, C. M.; Allen, S. D.; Lobkovsky, E. B.; Coates, G. W. Alternating Copolymerization of Limonene Oxide and Carbon Dioxide. *J. Am. Chem. Soc.* **2004**, *126* (37), 11404−11405.
(91) Lamparelli, D. H.; Grimaldi, I.; Martínez-Carrión, A.; Bravo, F.; Kleij, A. W. Supercritical CO_2 as an Efficient Medium for Macromolecular Carbonate Synthesis through Ring-Opening Co- and Teroligomerization. *ACS Sustain. Chem. Eng.* **2023**, *11* (22), 8193−8198.
(92) Wambach, A.; Agarwal, S.; Greiner, A. Synthesis of Biobased Polycarbonate by Copolymerization of Menth-2-ene Oxide and CO2 with Exceptional Thermal Stability. *ACS Sustain. Chem. Eng.* **2020**, *8* (39), 14690−14693.
(93) Arita, T.; Kayama, Y.; Ohno, K.; Tsujii, Y.; Fukuda, T. High-pressure atom transfer radical polymerization of methyl methacrylate for well-defined ultrahigh molecular-weight polymers. *Polymer* **2008**, *49* (10), 2426−2429.
(94) Kurtz, S. M. *UHMWPE Biomaterials Handbook: Ultra High Molecular Weight Polyethylene in Total Joint Replacement and Medical Devices*; Academic Press, 2009.
(95) Diodati, L. E.; Wong, A. J.; Lott, M. E.; Carter, A. G.; Sumerlin, B. S. Unraveling the Properties of Ultrahigh Molecular Weight Polyacrylates. *ACS Appl. Polym. Mater.* **2023**, *5*, 9714−9720.
(96) Hester, H. G.; Abel, B. A.; Coates, G. W. Ultra-High-Molecular-Weight Poly(Dioxolane): Enhancing the Mechanical Performance of a Chemically Recyclable Polymer. *J. Am. Chem. Soc.* **2023**, *145* (16), 8800−8804.

https://doi.org/10.1021/jacs.3c14170
J. Am. Chem. Soc. 2024, 146, 8381−8393